Biol. Cybern. 84, 217–226 (2001)

Biological Cybernetics

Analysis of kinematically redundant reaching movements using the equilibrium-point hypothesis

Paola Cesari[1,2], **Takako Shiratori**[1], **Paolo Olivato**[3], **Marcos Duarte**[4]

[1] Department of Kinesiology, The Pennsylvania State University, University Park, PA 16802
[2] CeBISM – Center of Bioengineer and Movement Science, Via M. Dal Ben 5/b, 38068 Rovereto, Italy
[3] I.S.E.F. – Istituto Superiore di Educazione Fisica, Verona, Italy
[4] Escola de Educação Fisica e Esporte, Universidade de São Paulo, Av. Mello Moraes 65, 05508-900, São Paulo/SP, Brazil

Received: 3 May 1999 / Accepted in revised form: 19 May 2000

Abstract. Six subjects performed a planar reaching arm movement to a target while unpredictable perturbations were applied to the endpoint; the perturbations consisted of pulling springs having different stiffness. Two conditions were applied; in the first, subjects had to reach for the target despite the perturbation, in the second condition, the subjects were asked to not correct the motion as a perturbation was applied. We analyzed the kinematics profiles of the three arm segments and, by means of inverse dynamics, calculated the joint torques. The framework of the equilibrium-point (EP) hypothesis, the λ model, allowed the reconstruction of the control variables, the "equilibrium trajectories", in the "do not correct" condition for the wrist and the elbow joints as well as for the end point final position, while for the other condition, the reconstruction was less reliable. The findings support and extend to a multiple-joint planar movement, the paradigm of the EP hypothesis along with the "do not correct" instruction.

1 Introduction

The equilibrium-point (EP) hypothesis (Feldman 1966, 1986) suggests that the central nervous system (CNS) controls voluntary movements of a limb, not by performing inverse dynamic calculations and generating appropriate joint torque patterns, but by manipulating equilibrium states of the system "limb plus load". An important feature of the hypothesis is that muscles are viewed, not as generators of force patterns, but rather as generators of elastic force fields, whose properties are manipulated in time by the CNS.

Originally, the EP hypothesis was introduced for the control of single muscles and the threshold of the tonic stretch reflex (λ) was suggested as the only central variable manipulated by the CNS to control a muscle. For a single muscle, the force field is unidirectional and is controlled with the single variable λ. Later, the hypothesis was generalized for control of pairs of muscles acting at a simple pin joint. The behavior of such a joint is defined by an interaction of external forces and the sum of force fields generated by the two muscles. The muscle-generated force fields can be described with two central variables, two λ values or another pair $\{r, c\}$ (Feldman 1986; Feldman and Levin 1995). In a linear approximation and in the steady state, the $\{r, c\}$ pair is related to the intercept and slope of the joint compliant characteristics (JCC), which is the sum of tonic stretch reflex characteristics of the two muscles controlling the joint (Latash 1993). For a multi-joint, kinematically redundant limb, two complex variables can be viewed as central control variables, one related to the instantaneous equilibrium position of the endpoint of the limb, and the other related to the stability of the endpoint in this equilibrium state (Mussa Ivaldi et al. 1985; Latash 1993; Latash et al. 1999). The problem of defining pairs of single-joint control variables $\{r, c\}$ based on values of the control variables for the endpoint of a kinematically redundant limb is generally ill-posed. In previous studies, patterns of hypothetical control variables were reconstructed during single-joint movements (Latash and Gottlieb 1991, 1992; Bellomo and Inbar 1997), two-joint movements during tasks performed by a non-redundant two-joint segment (Gomi and Kawato 1996, 1997; Latash et al. 1999), and whole-body movements within a constrained motor task also not including redundancy (Domen et al. 1999). In these experiments, subjects were typically asked to perform a standard motor task and "not to intervene" if external conditions of task execution changed. Note that it is much more natural for a human subject to react to an external perturbation than "not to intervene". The effects of the two instructions ("correct the movement" versus "do not intervene") were compared during single-joint movements and demonstrated higher coefficients of correlation between joint torque and angle under the "do not intervene" instruction, as expected within the EP hypothesis (Latash 1994).

Correspondence to: P. Cesari
(Tel.: +45-8952611, Fax: +45-8952631, e-mail: pcesari@univr.it)

Notice that control variables have never been reconstructed during movements in the presence of kinematic redundancy. Therefore, within these studies, we wanted to demonstrate that the framework of the EP hypothesis allows the reconstruction of the hypothetical control variables (''equilibrium trajectories'') for individual joints and for the endpoint during natural, reaching movements performed by a kinematically redundant limb. Besides, we wanted to compare the performance of subjects under the ''correct'' and ''do not intervene'' instructions during such a multi-joint task. Note that the presence of motor redundancy does not allow generalizing the findings of the previous study of single-joint movements.

2 Method

Six healthy volunteers, four men and two women, aged 25–74 years, participated in the study. The average mass and height were 72.9 ± 5.1 kg and 1.76 ± 0.08 m, respectively, for men and 53.5 ± 3.1 kg and 1.61 ± 0.01 m respectively, for women. All the subjects were right-handed and they had never participated in a similar experiment before. No subjects had any known history of a neurological or peripheral motor disorder; all the subjects provided informed consent prior to testing.

2.1 Apparatus

During the experiment, the subjects sat on a chair with a rigid back support, with their left arm resting on the left thigh; they were instructed to sit comfortably with their back against the support. The right arm was used to move a tennis ball from an initial position to a target. One end of an elastic band (a spring) was attached to the ball, while the other end was attached to the wall behind the subject. Five springs with five different coefficients of stiffness were used for this experiment; each spring resting length was 1 m. Each spring was calibrated prior to the experiment by applying known loads and measuring the resultant elongation. All the springs demonstrated linear relations between force and elongation within the range of elongation used, with the coefficients of linear correlation over 0.98. The stiffness coefficients of the springs were 9.8, 9.9, 14.6, 31.4, and 56.9 N/m.

An electromechanical trigger was mounted on the back support of the chair; its position was adjusted for each subject to shoulder height at a comfortable position. The chair was positioned so that the distance from the point of spring attachment to the wall to the initial position of the tennis ball was exactly 1 m. Thus, each movement started approximately at zero length of each spring. A rigid guide was put under the spring between the wall and the initial position, so that the weight of the spring did not affect its force in the horizontal direction. The subject grabbed the tennis ball and occupied the initial position pressing on the trigger with the dorsal part of the hand. The trigger was released as soon as the movement started; its release generated a signal triggering the recording of the data.

A target (a squared rigid panel of 10 cm × 10 cm) was mounted on an adjustable stand, and was positioned at shoulder height at 80% of the maximal arm extension for each subject. Kinematics data were collected by an optoelectronic system ELITE (BTS, Milano, Italy). Five reflective markers were attached to the following points on the right arm of the subjects: the acromion, the lateral epicondyle of humerus, the ulnar head, the distal part of the fifth metacarpal, and to the tennis ball. The trigger was electrically connected to the ELITE data acquisition box, which was then connected to an IBM compatible PC collecting the three-dimensional kinematics data at a sampling frequency of 100 Hz. The reaching movement studied here is a radial movement where the direction of movement and perturbations is a straight line intersecting the shoulder joint; such a task has been studied before for a two-link arm (McIntyre et al. 1996) and accentuates the problem of stability at the end-point.

2.2 Procedure

In all the trials, the subjects were instructed to move ''at their comfortable speed'' from the initial position to the target and to stop at the target. The target had dimension of 10 cm × 10 cm, such that accuracy was not strongly emphasized. The experiment started with a practice session. During this session, the subjects practiced movement of the tennis ball attached to the spring with the intermediate value of stiffness of 14.6 N/m (we will address this spring as ''the standard spring'') with eyes open and eyes closed for about 1 min. After the subjects were confident in their ability to produce a standard movement, they practiced movements against different springs under the instruction ''do not correct your movement if it happens to be inaccurate''. The five different springs were presented randomly and each subject moved against each spring at least twice so that the total number of practice trials were at least 10 with 4-s intervals between trials (the time needed to change the spring). After both the subject and the experimenter were satisfied with the subject's ability ''not to correct'' movements performed against different springs, the main body of the experiment started.

Two series of movements were recorded. Each series consisted of 24 movements; the series was divided in four blocks with 6 trials each; in between the blocks, the subjects were asked to perform 4 movements against the standard spring to make sure that no drift in performance occurred. The intervals between the trials within a block were approximately 4 s; the intervals between the blocks were approximately 10 s. There was a 20-min interval between the two series. In the first series, the subjects were asked to perform 24 movements against springs that were disconnected and reconnected prior to each movement so that the subject never knew against which spring he or she was going to move. The

instruction was "do not correct", the same as during the immediately preceding practice. Prior to the second series, the subjects received another practice session of at least 10 trials such that they moved against each spring at least twice. In this session, the subjects were asked to try to hit the target in each movement; we will refer to this instruction as "correct". Then, a 24-movement series was run under the "correct" instruction; similar to in the first series, the spring was disconnected and reconnected after each trial. The experiment took about 1 h for each subject and fatigue was never an issue.

The perturbations used here were present during the entire movement (about 500 ms). Here, we assumed that the subjects were able to suppress voluntary reactions in spite of such long perturbations (in the "do not correct" instruction). This assumption has also been the basis of other studies (Bennet et al. 1992; Latash 1993). An important characteristic of the perturbations, particularly for the prolonged ones, is that they must be of low amplitude. This is the reason for the low stiffness values of the springs used here as sources of perturbations.

2.3 Data analysis

All data were filtered by using a Lambda filter algorithm implemented in the ELITE system. This filter uses an autoregressive model fitted to the signal that allows the evaluation of the filter bandwidth; then, a low pass filtering is performed in the frequency domain by a linear phase FIR filter (D'Amico and Ferrigno 1990). Using the position data for the five markers, the angular and linear kinematics were computed, then a fourth-order and zero-lag low-pass Butterworth filter with a cut-off frequency of 6 Hz was used after the numerical differentiation. The analysis demonstrated that the data were mostly confined to a sagittal plane. For all trials, the displacement of the endpoint was performed in the anterior-posterior direction (see Fig. 1, the x-axis). The maximum displacement in the lateral and in the vertical directions were only up to 5% of the total endpoint displacement; all subsequent analyses were done considering the motion in the sagittal plane.

2.4 Joint torque calculation

To solve the inverse dynamic problem, we used a rigid body model in the sagittal plane with four segments (trunk, upper arm, forearm and hand) and three frictionless hinge joints (shoulder, elbow and wrist), as shown in Fig. 1. The equations of motion for the model using a Newton-Euler formulation are presented in the Appendix. The equations considered the following forces acting on the body segments: joint reactive forces, force of gravity, spring force and the linear and angular motion-dependent forces including the centripetal and the Coriolis forces. Muscle moments for each joint were computed as single net moment about each joint (Fig. 1). The body segment parameters were calculated based on anthropometric data using regression equations from Zatsiorsky et al. (1990). The values of these parameters are presented in Table 1.

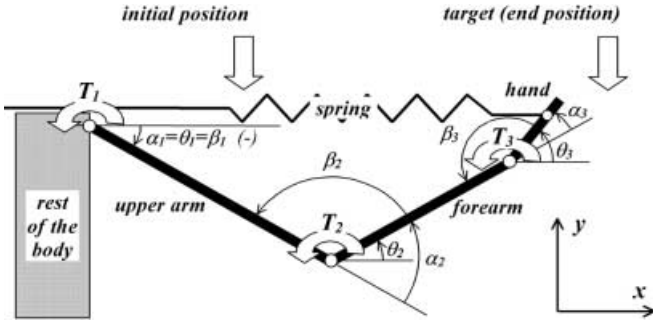

Fig. 1. Model of the human body for the arm movement in the sagittal plane with the schematic location of the initial and target position

2.5 Reconstruction of joint equilibrium trajectories

Our analysis was based on the following major assumptions.

(1) Under the instruction "do not correct", during each trial, the subject reproduces the same pattern of control variables for each joint.
(2) The equilibrium trajectory represents the outcome of a central command and it is derived from the patterns of two variables, $r(t)$ and $c(t)$ for each joint. These variables are defined according to the framework of the EP hypothesis (Feldman 1986; Latash 1993; Feldman and Levin 1995).
(3) Based on the EP hypothesis, the resultant torque at each joint generated by its spring-like muscles can be described with the linear model $T_i(t) = k_i(t) \cdot [\beta_i(t) - \beta_{0i}(t)]$, where the subscripts i refers to the joint i, $k(t)$ is time-varying stiffness, $\beta(t)$ is the joint angle, and $\beta_{0i}(t)$ is time-varying "zero length" value of the elastic element in the joint.

Table 1. Anthropometric parameters for the six subjects estimated using model of Zatsiorsky et al. (1990). The center of gravity location and moment of inertia were also estimated by the same model. L and M refer to the length and mass, respectively, of the body segments

Subject	L. upper arm [m]	L. forearm [m]	L. hand [m]	M. upper arm [kg]	M. forearm [kg]	M. hand [kg]
1	0.247	0.255	0.186	2.168	1.296	0.488
2	0.272	0.268	0.192	1.935	1.157	0.436
3	0.222	0.228	0.173	1.301	0.704	0.286
4	0.247	0.231	0.175	1.428	0.773	0.314
5	0.320	0.275	0.201	1.951	1.166	0.439
6	0.260	0.242	0.181	1.843	1.102	0.415

We assumed that damping torques were small and could be neglected. This assumption has been a point of controversy (Latash and Gottlieb 1991, 1992; Latash 1992; Feldman and Levin 1995; Gomi and Kawato 1997; Gribble et al. 1998). However, since in the present series of experiments, the subjects were moving at relatively low velocities (peak velocities in the range, for the elbow of 143–226 deg/s, for the wrist from −31.4 to −54.6 deg/s, i.e. with the peak velocities of very fast movements that are of the order of 500 deg/s; Gottlieb et al. 1991), damping forces were unlikely to play a major role.

We assumed that a pair of control functions $\{r(t), c(t)\}$ are reproduced across trials for each joint, corresponding to a learned movement against the standard spring. According to the EP hypothesis, a pair of values $\{r_1, c_1\}$ identifies a dependence of muscle torque upon joint angle, i.e. the location and slope of a JCC. Thus, if the subject is not correcting movements, or, in other words, reproducing the same time function $r(t)$ and $c(t)$, at any time t_i after the movement initiation, there exists a dependence between joint torque and angle common across all the trials. Changes in the external force provided by different springs changed actual kinematics so that, in different trials, at t_i, joint state could be characterized by different combinations of instantaneous torque and angle (T_i, β_i). However, all the (T_i, β_i) pairs are expected to belong to the same JCC. We assumed, for simplicity, a linear relation between joint torque and angle, similarly to previous studies with reconstruction of JCC during single-joint and two-joint movements (Latash 1993; Latash et al. 1999).

Note that this approach has been criticized for (1) using a linear model, (2) ignoring velocity-dependent torques and (3) ignoring time delays in the tonic stretch reflex loop (Feldman and Levin 1995; Gribble et al. 1998). However, we believe that these simplifications do not compromise the analysis of slow and smooth tasks, as in the present study, and allow the use of a very simple model.

Linear regression analyses were performed for each joint, for sets of points on the torque-angle plane every 50 ms starting from the movement initiation (trigger signal) until 600 ms. Each regression equation was used to calculate the instantaneous joint equilibrium position as the intercept of the regression line with the current external load (represented by linear regression of the values of the external load at each instant calculated by the inverse dynamics approach). The external load is considered to be the sum of the gravitational torque and the spring torque (the difference between the actual spring torque and the standard spring torque). The instantaneous joint equilibrium position is a position at which the joint would eventually come to rest if no further changes in control signals and external forces took place. An interpolation of instantaneous equilibrium positions was considered the joint equilibrium trajectory.

Equilibrium trajectories of the endpoint were reconstructed under the same major assumptions, using a single-dimensional model $F(t) = k(t) \cdot [x(t) - x_0(t)]$, where F is force acting on the endpoint (the tennis ball), x is the coordinate of the ball along the x-axis, x_0 is time varying "zero position" of the instantaneous elastic force field at time t, and k is the difference between the standard spring stiffness and the actual spring stiffness.

A series of trials performed under the other instruction ("always try to hit the target") was subjected to the same type of analysis. Note that, under this instruction, the subjects were expected to change their central commands after a certain delay. Therefore, the first of the earlier mentioned assumptions is violated, and we expected the method to work poorly after a certain reaction time delay.

3 Results

3.1 Kinematics and kinetic profiles

Due to the experimental design, the perturbation torques on the shoulder caused by the spring forces are minimal because the action lines pass approximately through the shoulder joint (see Fig. 1). Although the analysis was performed for the three joints, the results presented here refer only to the elbow and the wrist joints. Figure 2 illustrates typical kinematics and torque profiles for the elbow, wrist and the endpoint under the "do not correct" instruction for a representative subject. The weakest, standard, and strongest springs were used with stiffness of 9.8 N/m, 14.6 N/m, and 56.9 N/m, respectively. Note that the trigger acted when the movement was already under way so that the elbow velocity was about 25% of its peak value. Elbow movements were characterized by bell-shaped velocity profiles and double-peak accelerations while the wrist presented more complex profiles.

Table 2 shows the mean values and standard deviations for the five springs of the angular amplitudes and the peak angular velocities for the elbow and the wrist. Note the change in the elbow amplitude during movements against the two springs with the highest stiffness under the "do not correct" instruction. The differences from the amplitude during movement compared to the standard spring are statistically significant, (for springs 3 and 4, $t = 5.45$; for springs 4 and 5, $t = 8.73$, $p < 0.01$); while no statistical differences were present under the "correct" instruction. Peak velocities in the elbow dropped with an increase in spring stiffness under both instructions ($p < 0.01$). There were no significant changes in these kinematics indices for the wrist.

3.2 Patterns of equilibrium trajectories

As mentioned in Sect. 2, we used linear regression analyses to define instantaneous equilibrium positions in the joints and of the endpoint. Figure 3 illustrates typical scatters of data points and regression lines for a typical subject who performed movements under the "do not correct" instruction. Some scatters of data points showed low coefficients of correlation and did not allow reconstruction of an equilibrium point. We

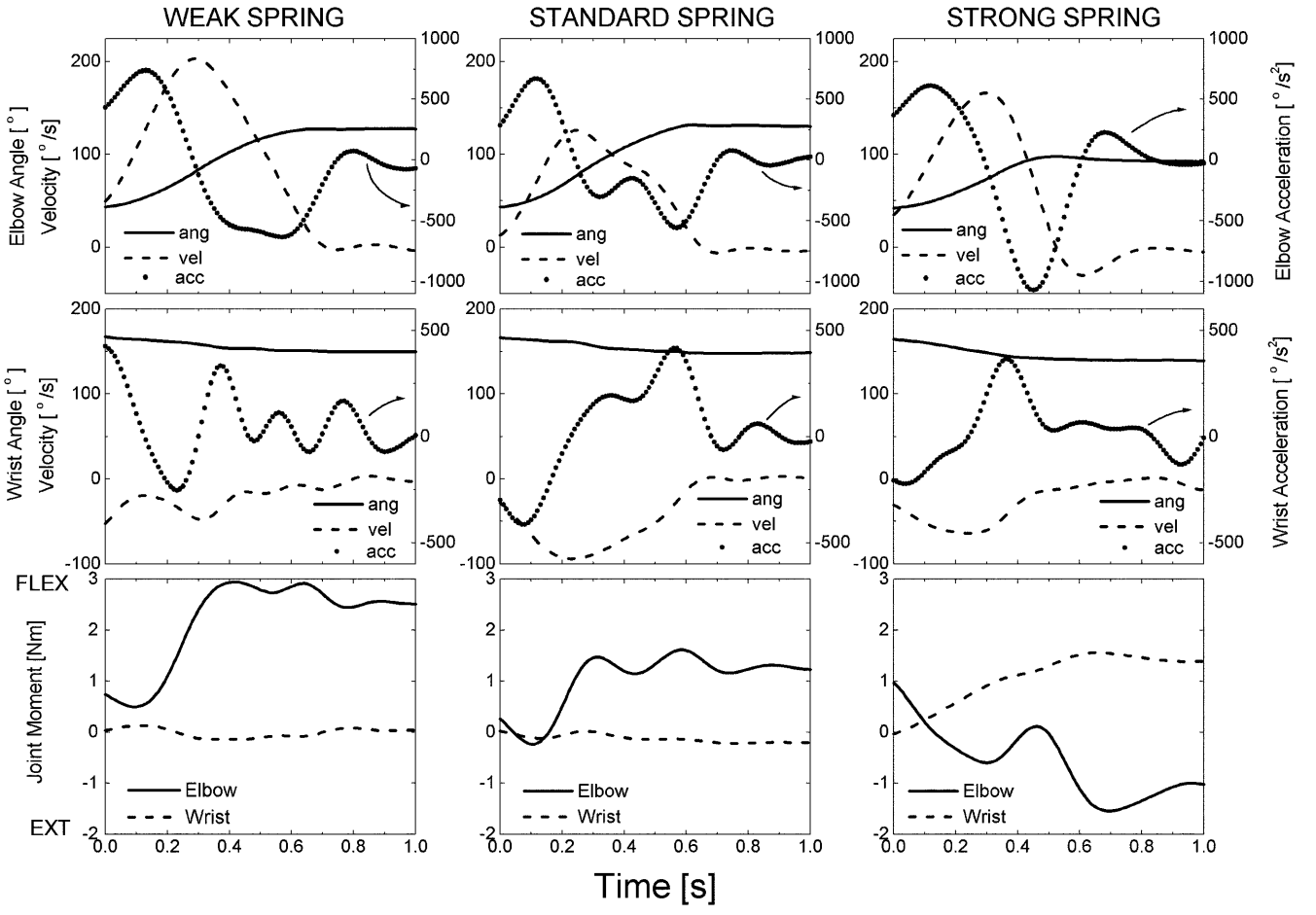

Fig. 2. Example of trajectories of angular displacements, velocities, and accelerations and joint torques of elbow and wrist for three different springs. The three springs represented are the weakest (9.8 N/m) the standard (14.6 N/m) and the strongest (56.9 N/m). Angle, ang; angular velocity, vel; angular acceleration, acc. Subject 5 in the "do not correct" instruction

Table 2. Average angular displacement and angular peak velocity for the elbow and wrist in function of different spring stiffness

Spring	Δang_{elbow} [°]	Δang_{wrist} [°]	$Vpeak_{elbow}$ [°/s]	$Vpeak_{wrist}$ [°/s]
"Do not correct"				
1	83.6 ± 16.9	10.7 ± 6.6	216.8 ± 59.4	−45.6 ± 19.7
2	83.2 ± 10.6	10.2 ± 6.3	211.1 ± 60.4	−39.1 ± 16.5
3	84.5 ± 10.7	10.7 ± 5.9	206.6 ± 46.6	−44.4 ± 21.8
4	66.3 ± 16.8	12.4 ± 7.4	170.5 ± 47.7	−31.4 ± 17.1
5	45.7 ± 16.7	11.7 ± 7.3	143.0 ± 48.9	−46.4 ± 25.6
"Correct"				
1	86.5 ± 10.3	11.8 ± 6.4	226.2 ± 41.5	−46.4 ± 34.5
2	86.7 ± 10.0	11.6 ± 7.6	219.0 ± 39.5	−52.4 ± 25.4
3	87.1 ± 10.5	12.9 ± 7.3	218.6 ± 47.0	−54.6 ± 28.5
4	89.3 ± 10.6	13.7 ± 9.3	192.3 ± 40.2	−46.5 ± 33.2
5	89.5 ± 10.6	14.2 ± 8.9	174.3 ± 46.2	−47.7 ± 24.3

accepted the following criterion: if the correlation coefficient was over the critical value for statistical significance at $p < 0.05$ ($r_{cr} = 0.36$ for 24 observations), the data set was accepted and the instantaneous equilibrium position was calculated. Typically, the correlation coefficient reached this critical value about 200 ms after the initiation of the movement. In order to perform simple statistics and testing hypotheses, the correlation coefficients were transformed to Z values (Sokal and Rohlf 1981).

Table 3 shows the mean values and the standard deviations of Z values computed based on correlation coefficients for each subject for the elbow joint, the wrist joint, and the end point across all time slices. Five out of six subjects showed higher correlation coefficients for the elbow data for the "do not correct" instruction with

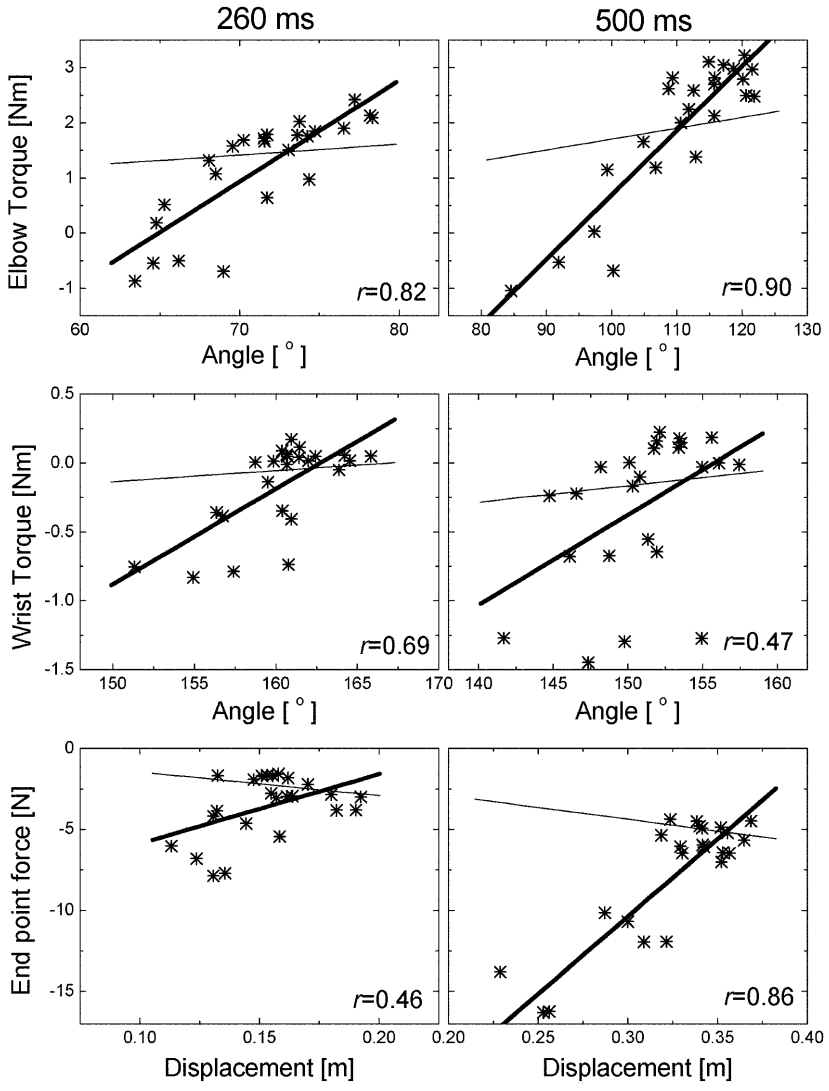

Fig. 3. Example of elbow, wrist and end point scatter points and linear regression and coefficient of correlation for two different instants after the motion onset: 260 ms and 500 ms. The *thin lines* represent linear regressions of the external loads so that the intersection between the thin line and the regression line (*bold*) in each plot gives the instantaneous equilibrium position. Subject 5 in the "do not correct" instruction

Table 3. Average correlation coefficients for elbow, wrist and end point final trajectories for each subject across all time slices

Subject	Elbow	Wrist	End point
"Do not correct"			
1	0.87 ± 0.34	0.71 ± 0.07	0.46 ± 0.12
2	0.71 ± 0.26	0.46 ± 0.10	0.26 ± 0.09
3	0.83 ± 0.39	0.08 ± 0.09	0.65 ± 0.42
4	0.63 ± 0.13	0.42 ± 0.05	0.32 ± 0.34
5	0.82 ± 0.14	0.60 ± 0.14	0.77 ± 0.32
6	0.46 ± 0.25	0.11 ± 0.15	0.10 ± 0.16
Mean ± SD	0.75 ± 0.24	0.43 ± 0.05	0.46 ± 0.21
"Correct"			
1	0.85 ± 0.19	0.64 ± 0.15	0.57 ± 0.19
2	0.60 ± 0.09	0.56 ± 0.07	0.35 ± 0.26
3	0.43 ± 0.07	0.07 ± 0.05	0.13 ± 0.19
4	0.72 ± 0.14	0.47 ± 0.13	0.59 ± 0.39
5	0.74 ± 0.06	0.29 ± 0.09	0.59 ± 0.23
6	0.66 ± 0.03	0.23 ± 0.10	0.16 ± 0.21
Mean ± SD	0.69 ± 0.06	0.39 ± 0.07	0.38 ± 0.25

respect to the "correct" instruction (Table 3); overall, the data for the wrist and for the end point were much more variable.

Equilibrium trajectories were reconstructed as interpolations of instantaneous equilibrium positions. Figure 4 shows the elbow, wrist, and end point trajectories for each subject. Notice again the better reproducible trajectory for the elbow as compared to the wrist. The wrist trajectories for two subjects are missing due to the low values of the correlation coefficients.

The correlation coefficients for all subjects at different instants after t_0 were calculated for both instructions (see Table 4) and transformed in Z values. Figure 5 shows the plot of the Z values for the elbow across time for each subject. Notice that, after a certain period which varied for each subjects, the Z values for the "do not correct" instruction were higher and the patterns representing the two instructions became separated.

The instant when the two patterns separated more markedly took place before 400 ms for four subjects and around 500 ms for two subjects. A similar trend was observed for the Z values calculated for the wrist and for the end point data.

The values of the stiffness calculated for each joint and the endpoint of the reconstructed equilibrium trajectories in the "do not correct" instruction were

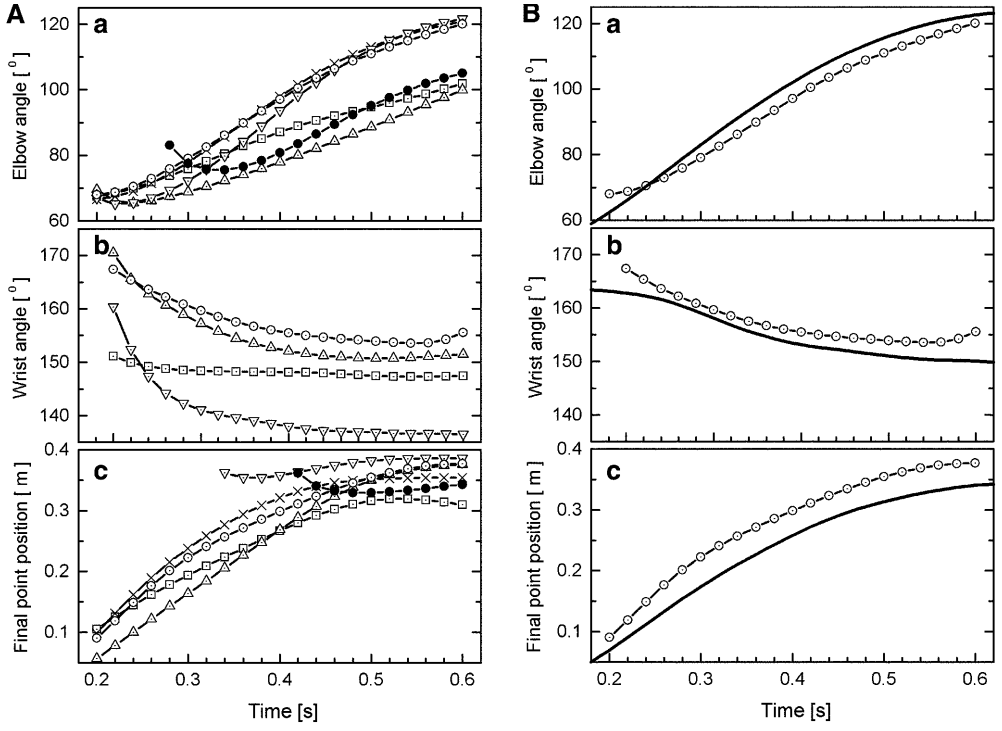

Fig. 4. **A** Equilibrium trajectories, for all the subjects: subject 1, *square*; subject 2, *up triangle*; subject 3, *cross*; subject 4, *down triangle*; subject 5, *open circle*; subject 6, *solid circle* in the "do not correct" instruction. (a) elbow, (b) wrist, and (c) end point. Note that, for some subjects, some points or the whole trajectory is missing due to the low value of the correlation coefficient. **B** Equilibrium trajectories of subject 5 (*open circles*) and average actual trajectories of the eight trials with the standard spring in the "do not correct" instruction (*bold lines*)

Table 4. Average correlation coefficients for elbow, wrist and end point final trajectories for each instant

Instant [%]	Elbow	Wrist	End point
"Do not correct"			
0	0.62 ± 0.34	0.49 ± 0.27	0.23 ± 0.24
25	0.66 ± 0.26	0.42 ± 0.35	0.35 ± 0.32
50	0.72 ± 0.30	0.40 ± 0.35	0.47 ± 0.37
75	0.80 ± 0.36	0.40 ± 0.33	0.56 ± 0.42
100	0.87 ± 0.38	0.41 ± 0.27	0.64 ± 0.45
Mean ± SD	0.75 ± 0.33	0.43 ± 0.32	0.46 ± 0.36
"Correct"			
0	0.64 ± 0.20	0.48 ± 0.26	0.12 ± 0.16
25	0.67 ± 0.24	0.41 ± 0.26	0.22 ± 0.23
50	0.69 ± 0.28	0.37 ± 0.27	0.35 ± 0.33
75	0.71 ± 0.33	0.37 ± 0.27	0.52 ± 0.32
100	0.71 ± 0.32	0.33 ± 0.24	0.63 ± 0.31
Mean ± SD	0.69 ± 0.27	0.39 ± 0.26	0.38 ± 0.27

approximately the same for all subjects and presented a monotonic increase for all except for one subject. Figure 6 shows the time evolution of the average stiffness of all subjects in the "do not correct" instruction. Across time and for all subjects, the values of the stiffness were 6.5 ± 2.2 Nm/rad for the shoulder, 4.3 ± 1.9 Nm/rad for the elbow, 2.1 ± 1.3 Nm/rad for the wrist, and 17.4 ± 12.2 N/m for the endpoint with peak values about twice these respective values.

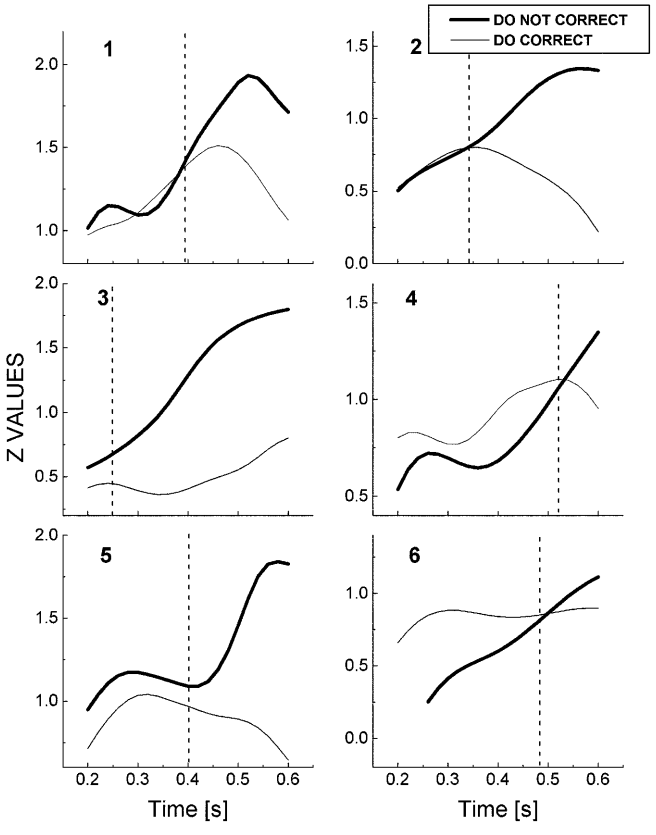

Fig. 5. Plots of the *Z*-value transformation of the correlation coefficients versus time for the elbow joint under both instructions for each subject. The *bold lines* refer to the "do not correct" instruction while the *thin lines* are for the "correct" instruction. Significance of the difference between the two curves starting at the vertical lines: $^{*}p < 0.05$, $^{**}p < 0.001$

4 Discussion

The main result of the present study is the demonstration of a possibility to reconstruct the "equilibrium

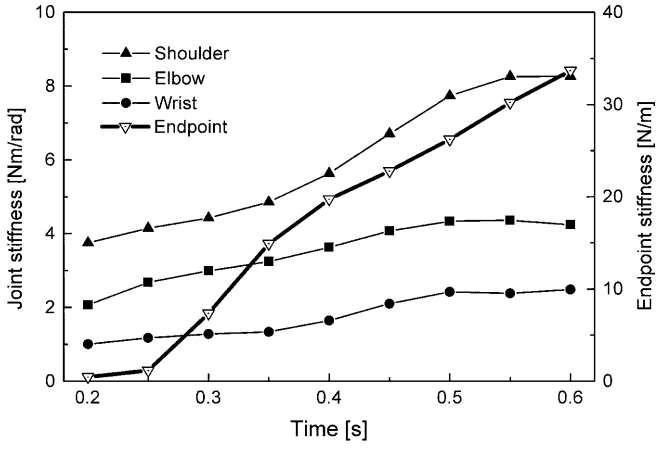

Fig. 6. Time evolution of the shoulder, elbow, wrist, and endpoint stiffness average values of the reconstructed equilibrium trajectories in the "do not correct" instruction for all subjects

trajectories" of individual joints as well as of the final position of the endpoint during a natural reaching movement. In particular, we demonstrate that the reconstruction is possible by considering a multi-joint (in this case, three-joint) movement performed following the "do not correct" instruction. The "do not correct" instruction has been a major point for the EP hypothesis which assume that subjects interpret the instruction so as to apply the "same central command" (Feldman and Levin 1995; Mussa-Ivaldi et al. 1985). The rational under this assumption is that, if this is the case, we should observe a linear relationship in our model between the movement parameters (torque-angle) and the perturbation applied. This type of instruction was never tested in a multi-joint movement.

4.1 The comparison between the two instructions

Our main point for testing the same task under two different instructions was to show that subjects used two different movement strategies and that the framework of the EP hypothesis was only applicable under the "do not correct" instruction as previously shown (Latash 1994). A clear result that corroborates the distinction between the two instructions is by comparing their kinematic profiles and, in particular, the different angle amplitudes expressed at the elbow joint. In addition, differences in behavior between the two instructions were supported by the different goodness of fit values defined by the Z value, which in the "do not correct" instruction showed a systematic greater increase for all the subjects.

It is interesting to notice that, in both instructions, each individual showed different instances of Z value increases, indicating that the perturbation applied was perceived by each subject differently. The significance of the difference between the two curves starting at the time slice indicated by the vertical lines (Fig. 5) was tested by a t-test for paired samples. Five out of the six subjects showed a significant difference between the two curves ($p < 0.05$).

4.2 The "do not correct" instruction

By considering the results for the "do not correct" instruction, we were able to reconstruct all the equilibrium trajectories for the elbow but not for the wrist joint. A possible explanation for the two different joint patterns could be that the wrist is not the focal joint involved in the accomplishment of this task, a fact corroborated by the small range of movement observed for the wrist (similar findings have been reported by two-joint movements: (Latash et al. 1999). Another possibility is that, to simplify the control and accomplish the task, the CNS prefers not to use the wrist joint actuator and freezes this joint; this point will be discussed later. In the EP-hypothesis framework (Latash 1993; Latash et al. 1999) for a multi-joint movement, the control of the motion has been related primarily to the equilibrium state of the endpoint; for this reason, we expected to find a better reconstruction for the endpoint trajectory than for the wrist and the elbow trajectories. On the contrary, our results, (Tables 3 and 4) showed a better reconstruction for the elbow trajectory than the endpoint trajectory, suggesting once more that the elbow joint is the focal joint in such a task.

All the equilibrium trajectories presented a smooth and monotonic shape. Latash and Gottlieb (1992) proposed that for fast movements an N-shaped EP trajectory should account for the observed smooth real trajectories. The N-shaped profile is given by first accelerating, then decelerating the EP trajectory. However, Gribble et al. (1998) showed that when passive properties of the muscles are taken into account, simple EP trajectories are sufficient to generate smooth movements. The fact that we did not observed the N-shaped profile, even without considering the passive properties of the muscles, is due to the consistent low movement speed observed for all the subjects. In addition, the incremental opposing force to the end point generated by the springs decelerated the movement. The stiffnesses, 6.5 ± 2.2 Nm/rad for the shoulder and 4.3 ± 1.9 Nm/rad for the elbow, are comparable to the lowest values reported in the literature (Gomi and Kawato 1995). The statistically significant coefficients of correlation for the linear regression between torques and the corresponding joints indicate that the use of a linear model for the torque/joint relationship as well as the disregard of the viscosity component were not detrimental to the results.

4.3 The mechanics of the task

All the subjects presented a very small angular movement of the wrist joint compared to the movements of the other two joints. This limited movement excursion of the wrist joint could be viewed as a strategy of the CNS in applying a simplified control of the movement by directing the commands mainly to the shoulder and elbow joints. Due to the small movement of the wrist, the system can be simplified as a two-link system where the body segments, upper arm and arm plus hand, have approximately the same lengths. In addition, since a

radial movement was performed, the Coriolis torque cancels the centripetal torque for the shoulder joint (Hollerbach and Flash 1982) and the shoulder angle (β_S) is related to the elbow angle (β_E) by $2\beta_S + \beta_E = 180°$. As a result, there are no coupling terms acting on the shoulder joint and it behaves like a single-joint movement. As a consequence, this two-link system can be represented as a polar manipulator with no interaction between the two actuators (Mussa-Ivaldi 1986), and the shoulder stiffness is predicted to be twice the value of the interaction stiffness term[1] independent of the elbow stiffness value. Then, the number of independent terms in the stiffness matrix for a radial movement drops from three to two, which simplifies the control of the task in the framework of the EP hypothesis. This result is not straightforward because the CNS could have used the wrist joint movements to change the inertia to control the task, as shown by Hogan (1985) as an alternative strategy to an impedance controller. The method for estimation of the joint stiffness used here does not allow the estimation of the interaction stiffness terms but, as discussed above, for the particular movement studied, they can be estimated as being half of the shoulder stiffness. In general, we conclude that these findings cannot be extended to all kinematically redundant tasks since they represent the special case of a reaching radial movement.

Appendix

The following convention applies to the notation used in this paper. Subscript i runs 1, 2, or 3 meaning shoulder, elbow, or wrist joint when referring to angles, joint moments, or joint reaction forces, respectively, or meaning upper arm, forearm, or hand segment respectively, when referring to everything else.

x_i, y_i refer to the position of the center of mass of segment i in the horizontal or vertical directions, respectively.

l_i is the length of segment i. d_i is the distance from the proximal joint of the segment i to its center of mass position. d_S is the distance from the wrist joint to the point of application of the spring force. m_i is the mass of segment i. I_i is the moment of inertia of segment i. F_{xi}, F_{yi} are the joint reaction forces of joint i in the horizontal or vertical directions, respectively. F_S is the spring force. T_i is the joint moment of joint i. g is the gravitational acceleration.

Based on the model used here (see Fig. 1) the following relation applies to angles α, β, and θ.

$$\begin{aligned} &\alpha_1 = \beta_1 = \theta_1(-) \\ &\alpha_2 = \theta_2 - \alpha_1 \qquad \beta_2 = \pi - \alpha_2 \\ &\alpha_3 = \theta_3 - \alpha_2 - \alpha_1 \quad \beta_3 = \pi - \alpha_3 \ , \end{aligned} \tag{1}$$

α_i and β_i are the angles in the "joint space", β_i is the internal angle of joint i and α_I the external angle; θ_i is the angle of joint i in the "segment space".

In order to compute the equations of motion, the linear accelerations of the center of gravity of each link, taking into account the constraints imposed by the kinematics of the linkage and starting from the shoulder joint as a fixed reference point, were calculated by the first derivate of the Jacobian, J, of the angular velocities, or in a formal matrix form:

$$[\ddot{x}_i \ \ddot{y}_i]^{\mathrm{T}} = \dot{J}_i[\dot{\alpha}_1 \ \dot{\alpha}_2 \ \dot{\alpha}_3]^{\mathrm{T}} + J_i[\ddot{\alpha}_1 \ \ddot{\alpha}_2 \ \ddot{\alpha}_3]^{\mathrm{T}} \quad i = 1 \ldots 3 \ . \tag{2}$$

Based on the free body diagrams for Fig. 1, the equations of motion in the sagittal plane were derived by means of the Newton-Euler method. The joint moments can be expressed in the matrix-vector form:

$$T = M(\alpha)\ddot{\alpha} + v(\alpha, \dot{\alpha}) + G(\alpha) + T_{\mathrm{ext}} \ , \tag{3}$$

where T is the vector of joint moments (3×1), $M(\alpha)$ is the inertia matrix (3×3), $\ddot{\alpha}$ is the vector of angular accelerations (3×1), $v(\alpha, \dot{\alpha})$ is the vector of centrifugal/Coriolis terms (3×1), $G(\alpha)$ is the vector of gravity terms (3×1), T_{ext} is the vector of joint moments due to other external forces besides gravity; in this case, represents the moment due to the spring force (3×1).

The motion equations were rearranged in the above format and the correspondent terms are:

$$T = [T_1 \ T_2 \ T_3]^{\mathrm{T}} \ , \tag{4}$$

$$\ddot{\alpha} = [\ddot{\alpha}_1 \ \ddot{\alpha}_2 \ \ddot{\alpha}_3]^{\mathrm{T}} \ , \tag{5}$$

$$\begin{aligned} M(\alpha)_{1,1} = {} & m_1 d_1^2 + I_1 + m_2(\ell_1^2 + d_2^2 + 2\ell_1 d_2 \cos\alpha_2) + I_2 \\ & + m_3[\ell_1^2 + \ell_2^2 + d_3^2 + 2\ell_1\ell_2 \cos\alpha_2 \\ & + 2\ell_1 d_3 \cos(\alpha_2 + \alpha_3) + 2\ell_2 d_3 \cos\alpha_3] + I_3 \ , \end{aligned} \tag{6}$$

$$\begin{aligned} M(\alpha)_{1,2} = {} & m_2(d_2^2 + \ell_1 d_2 \cos\alpha_2) + I_2 + m_3[\ell_2^2 + d_3^2 \\ & + \ell_1\ell_2 \cos\alpha_2 + \ell_1 d_3 \cos(\alpha_2 + \alpha_3) \\ & + 2\ell_2 d_3 \cos\alpha_3] + I_3 \ , \end{aligned} \tag{7}$$

$$M(\alpha)_{1,3} = m_3[d_3^2 + \ell_1 d_3 \cos(\alpha_2 + \alpha_3) + \ell_2 d_3 \cos\alpha_3] + I_3 \ , \tag{8}$$

$$M(\alpha)_{2,1} = M(\alpha)_{1,2} \ , \tag{9}$$

$$M(\alpha)_{2,2} = m_2 d_2^2 + I_2 + m_3(\ell_2^2 + d_3^2 + 2\ell_2 d_3 \cos\alpha_3) + I_3 \ , \tag{10}$$

$$M(\alpha)_{2,3} = m_3(d_3^2 + \ell_2 d_3 \cos\alpha_3) + I_3 \ , \tag{11}$$

$$M(\alpha)_{3,1} = M(\alpha)_{1,3} \ , \tag{12}$$

[1] The stiffness interaction terms (the off-diagonal terms) have the same value due to the spring-like behaviour of the neuromuscular system generating a conservative force field during reaching tasks meaning that there are three independent terms in the 2×2 stiffness matrix in a general planar movement (Hogan 1985).

$$M(\alpha)_{3,2} = M(\alpha)_{2,3} \ , \tag{13}$$

$$M(\alpha)_{3,3} = m_3 d_3^2 + I_3 \ , \tag{14}$$

$$\begin{aligned} v(\alpha,\dot{\alpha})_1 = & -[(m_2\ell_1 d_2 + m_3\ell_1\ell_2)\sin\alpha_2 \\ & + m_3\ell_1 d_3 \sin(\alpha_2+\alpha_3)](2\dot{\alpha}_1\dot{\alpha}_2 + \dot{\alpha}_2^2) \\ & - [m_3\ell_1 d_3 \sin(\alpha_2+\alpha_3) + m_3\ell_2 d_3 \sin\alpha_3] \\ & \times (2\dot{\alpha}_1\dot{\alpha}_3 + 2\dot{\alpha}_2\dot{\alpha}_3 + \dot{\alpha}_3^2) \ , \end{aligned} \tag{15}$$

$$\begin{aligned} v(\alpha,\dot{\alpha})_2 = & [(m_3\ell_1\ell_2 + m_2 d_2\ell_1)\sin\alpha_2 \\ & + m_3 d_3\ell_1 \sin(\alpha_2+\alpha_3)]\dot{\alpha}_1^2 \\ & - m_3 d_3\ell_2 \sin\alpha_3(2\dot{\alpha}_1\dot{\alpha}_3 + 2\dot{\alpha}_2\dot{\alpha}_3 + \dot{\alpha}_3^2) \ , \end{aligned} \tag{16}$$

$$\begin{aligned} v(\alpha,\dot{\alpha})_3 = & [m_3\ell_1 d_3 \sin(\alpha_2+\alpha_3) + m_3\ell_2 d_3 \sin\alpha_3]\dot{\alpha}_1^2 \\ & + m_3\ell_2 d_3 \sin\alpha_3(2\dot{\alpha}_1\dot{\alpha}_2 + \dot{\alpha}_2^2) \ , \end{aligned} \tag{17}$$

$$\begin{aligned} G(\alpha)_1 = & \ m_1 g d_1 \cos\alpha_1 + m_2 g[\ell_1\cos\alpha_1 + d_2\cos(\alpha_1+\alpha_2)] \\ & + m_3 g[\ell_1\cos\alpha_1 + \ell_2\cos(\alpha_1+\alpha_2) \\ & + d_3\cos(\alpha_1+\alpha_2+\alpha_3)] \ , \end{aligned} \tag{18}$$

$$\begin{aligned} G(\alpha)_2 = & \ m_2 g d_2\cos(\alpha_1+\alpha_2) + m_3 g[\ell_2\cos(\alpha_1+\alpha_2) \\ & + d_3\cos(\alpha_1+\alpha_2+\alpha_3)] \ , \end{aligned} \tag{19}$$

$$G(\alpha)_3 = m_3 g d_3 \cos(\alpha_1+\alpha_2+\alpha_3) \ , \tag{20}$$

$$\begin{aligned} T_{\text{ext}}(\alpha)_1 = & -F_S\ell_1\sin\alpha_1 - F_S\ell_2\sin(\alpha_1+\alpha_2) \\ & - F_S(d_3+d_S)\sin(\alpha_1+\alpha_2+\alpha_3) \ , \end{aligned} \tag{21}$$

$$\begin{aligned} T_{\text{ext}}(\alpha)_2 = & -F_S\ell_2\sin(\alpha_1+\alpha_2) \\ & - F_S(d_3+d_S)\sin(\alpha_1+\alpha_2+\alpha_3) \ , \end{aligned} \tag{22}$$

$$T_{\text{ext}}(\alpha)_3 = -F_S(d_3+d_S)\sin(\alpha_1+\alpha_2+\alpha_3) \ . \tag{23}$$

Acknowledgements. The authors are very thankful to the Laboratory of Biomechanics in I.S.E.F., Verona, Italy, where the experimental part of this paper was performed. M. Duarte is thankful to Fundação de Amparo a Pesquisa do Estado de São Paulo (FAPESP/Brazil) for his post-doctoral scholarship. The authors greatly appreciate the comments of M. Latash in preparing the manuscript. This work was in part supported by a NIH grant NS-35032.

References

Bellomo A, Inbar G (1997) Examination of the λ equilibrium point hypothesis when applied to single degree of freedom movements performed with different inertial loads. Biol Cybern 76: 63–72

Bennet DJ, Hollerbach JM, Xu Y, Hunter IW (1992) Time-varying stiffness of the human elbow joint during cyclic voluntary movement. Exp Brain Res 88: 433–442

D'Amico M, Ferrigno G (1990) Technique for the evaluation of derivatives from noisy biomechanical displacement data using a model-based bandwidth-selection procedure. Med Biol Eng Comput 28: 407–415

Domen K, Latash ML, Zatsiorsky VM (1999) Reconstruction of equilibrium trajectories during whole-body movements. Biol Cybern 80: 195–204

Feldman A (1966) Functional tuning of the nervous system with control of movement or maintenance of a steady posture II. Controllable parameters of the muscle. Biophysics 11: 565–578

Feldman A (1986) Once more on the equilibrium point hypothesis (λ model) for motor control. J Mot Behav 18: 17–54

Feldman A, Levin M (1995) The origin and use of positional frames of reference in motor control. Behav Brain Sci 18: 723–804

Gomi H, Kawato M (1995) Task dependent stiffness of human-joint arm during point-to-point movement. Nippon Telegraph and Telephone ISRL-95-4

Gomi H, Kawato M (1996) Equilibrium-point control hypothesis examined by measured arm-stiffness during multi-joint movement. Science 272: 117–120

Gomi H, Kawato M (1997) Human arm stiffness and equilibrium-point trajectory during multi-joint movement. Biol Cybern 76: 163–171

Gottlieb GL, Corcos DM, Agarwal GC (1991) Strategies for the control of voluntary movements with one mechanical degree of freedom. Behav Brain Sci 14: 352–352

Gribble PL, Ostry DJ, Sanguineti V, Laboissière R (1998) Are complex control signals required for human arm movement? J Neurophysiol 79: 1409–1424

Hogan N (1985) The mechanics of multi-joint posture and movement control. Biol Cybern 52: 315–331

Hollerbach JM, Flash T (1982) Dynamics interactions between limb segments during planar arm movement. Biol Cyern 44: 67–77

Latash M (1992) Independent control of joint stiffness in the framework of the equilibrium point hypothesis. Biol Cybern 67: 377–384

Latash M (1993) Control of human movement. Human Kinetics Publishers, Illinois

Latash M (1994) Reconstruction of equilibrium trajectories and joint stiffness patterns during single-joint voluntary movements under different instructions. Biol Cybern 71: 441–450

Latash M, Gottlieb G (1991) Reconstruction of joint compliant characteristics during fast and slow movements. Neuroscience 43: 697–712

Latash M, Gottlieb G (1992) Virtual trajectories of single-joint movements performed under two basic strategies. Neuroscience 47: 357–365

Latash M, Aruin AS, Zatsiorsky VM (1999) The basis of a simple synergy: reconstruction of joint equilibrium trajectories during unrestrained arm movements. Hum Mov Sci 18: 3–30

McIntyre J, Mussa-Ivaldi FA, Bizzi E (1996) The control of stable postures in the multijoint arm. Exp Brain Res 110: 248–264

Mussa-Ivaldi FA (1986) Compliance. In: Morasso P, Tagliasco V (eds) Human movement understanding. North-Holland, Amsterdam

Mussa-Ivaldi FA, Hogan N, Bizzi E (1985) Neural, mechanical, and geometric factors subserving arm posture in humans. J Neurosci 5: 2732–2743

Sokal RR, Rohlf FJ (1981) Biometry: the principles and practice of statistics in biological research, 2nd edn., Freeman WH, San Francisco

Zatsiorsky VM, Seluyanov VN, Chugunova LG (1990) Methods of determining mass-inertial characteristics of human body segments. In: Chernyui GG, Regirer SA (eds) Contemporary problems of biomechanics, CRS Press, Boston